Activation and Coupling of the Glutaminase and Synthase Reaction of Glutamate Synthase Is Mediated by E1013 of the Ferredoxin-Dependent Enzyme, Belonging to Loop 4 of the Synthase Domain†

Laura Dossena, Bruno Curti, and Maria A. Vanoni*

Dipartimento di Scienze Biomolecolari e Biotecnologie, Università degli Studi di Milano, Via Celoria 26, 20133 Milano, Italy

Received September 7, 2006; Revised Manuscript Received January 31, 2007

ABSTRACT: Crystal structures of glutamate synthase suggested that a conserved glutamyl residue of the synthase domain (E1013 of *Synechocystis* sp. PCC 6803 ferredoxin-dependent glutamate synthase, FdGltS) may play a key role in activating glutamine binding and hydrolysis and ammonia transfer to the synthase site in this amidotransferase, in response to the ligation and redox state of the synthase site. The E1013D, N, and A, variants of FdGltS were overproduced in *Escherichia coli* cells, purified, and characterized. The amino acyl substitutions had no effect on the reactivity of the synthase site nor on the interaction with ferredoxin. On the contrary, a dramatic decrease of activity was observed with the D (∼100-fold), N and A (∼10000-fold) variants, mainly due to an effect on the maximum velocity of the reaction. The E1013D variant showed coupling between glutamine hydrolysis at the glutaminase site and 2-oxoglutarate-dependent L-glutamate synthesis at the synthase site, but a sigmoid dependence of initial velocity on L-glutamine concentration. The E1013N variant exhibited hyperbolic kinetics, but the velocity of glutamine hydrolysis was twice that of glutamate synthesis from 2-oxoglutarate at the synthase site. These results are consistent with the proposed role of E1013 in signaling the presence of 2-oxoglutarate (and reducing equivalents) at the synthase site to the glutaminase site in order to activate it and to promote ammonia transfer to the synthase site through the ammonia tunnel. The sigmoid dependence of the initial velocity of the glutamate synthase reaction of the E1013D mutant on glutamine concentration provides evidence for a participation of glutamine in the activation of glutamate synthase during the catalytic cycle.

Glutamate synthases (GltS[1]) are complex iron−sulfur flavoproteins found in microorganisms, plants, and lower animals. They catalyze the reductive L-glutamate (L-Glu) synthesis from L-glutamine (L-Gln) and 2-oxoglutarate (2-OG) through the coordination of activities that take place at catalytic subsites located on different enzyme domains and subunits (*1*−*4*, Figure 1).

L-Glu synthesis takes place in the synthase site where 2-OG binds in front of the FMN cofactor where it is suitably positioned for addition of an ammonia molecule to yield the postulated 2-iminoglutarate (2-IG) intermediate. This compound is then reduced to L-Glu with reduced FMN acting as the electron donor. The ammonia molecule is released upon L-glutamine hydrolysis at the glutaminase site, harbored within the type II glutamine amidotransferase (GAT) domain of GltS (Figure 1). The GAT and the synthase domains are located within the single polypeptide chain of FdGltS (Figures 1 and 2) and the corresponding α subunit of the NADPH-dependent bacterial enzyme (NADPH-GltS). These proteins share, with the well-characterized amidotransferases, the presence of an intramolecular tunnel for ammonia transfer from the glutaminase to the synthase site, which spans approximately 30 Å in FdGltS (*2*).

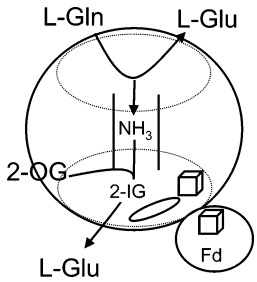

FIGURE 1: Model of the Fd-dependent glutamate synthase and distribution of catalytic subsites. The dotted ovals indicate the glutamine amidotransferase and the synthase domains of the FdGltS. The single oval represents FMN. The cubes indicate the GltS [3Fe-4S]$^{0,+1}$ cluster and the Fd [4Fe-4S]$^{+1,+2}$ cluster.

† This work was carried out with funds from Ministero dell'Istruzione, dell'Università e della Ricerca (Rome, Italy): PRIN2003, PRIN2005, and FIRST2003-2006.

* Corresponding author. Dipartimento di Scienze Biomolecolari e Biotecnologie, Università degli Studi di Milano, Via Celoria 26, 20133 Milano, Italy. Phone: +39-0250314901. Fax: +39-0250314895. E-mail: maria.vanoni@unimi.it.

[1] Abbreviations: 2-IG, 2-iminoglutarate; DON, 6-diazo-5-oxo-L-norleucine; FAD, flavin adenine dinucleotide; FdGltS, ferredoxin-dependent GltS; 2-OG, 2-oxoglutarate; Fd, ferredoxin; FMN, flavin mononucleotide; F6P, fructose-6-phosphate; GAT, L-glutamine-dependent amidotransferase; Glc6P, glucosamine-6-phosphate; GlmS, glucosamine-6-phosphate synthase; GltS, glutamate synthase; K_d, dissociation constant; INT, iodonitrotetrazolium, 2-(4-iodophenyl)-3-(4-nitrophenyl)-5-phenyltetrazolium chloride; MetS, L-methionine sulfone; MV, methyl viologen; NADPH, reduced nicotinamide-adenine dinucleotide phosphate; NADPH-GltS, NADPH-dependent GltS; ONL, 5-oxo-L-norleucine; TCA, trichloroacetic acid; *v*, initial velocity; *V*, apparent maximum velocity; *K* or K_M, apparent Michaelis constant.

10.1021/bi061865d CCC: $37.00
Published on Web 03/21/2007

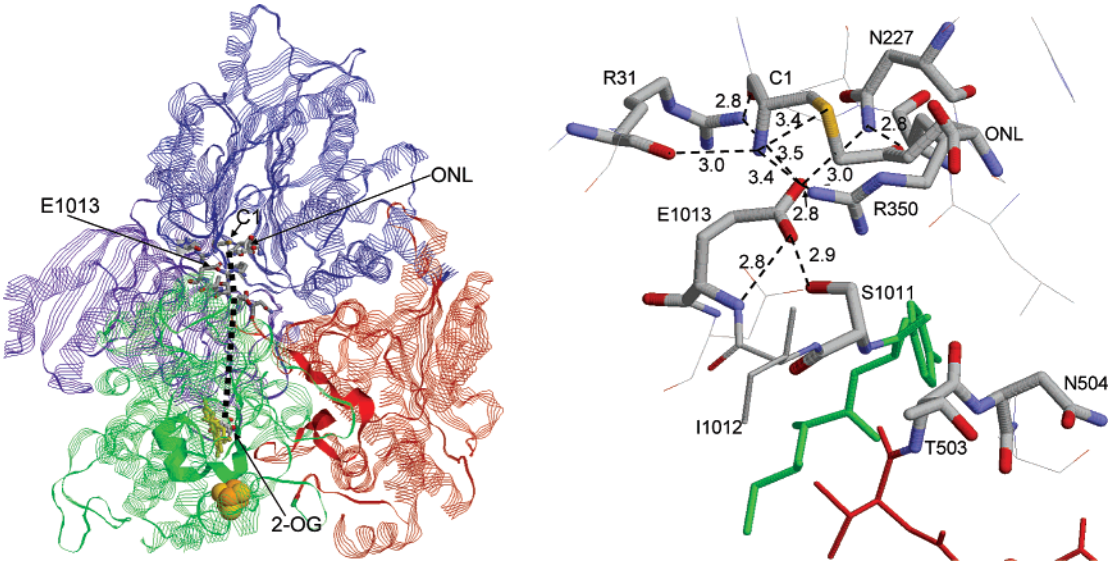

FIGURE 2: Structural model of FdGltS and details of the glutaminase site. Left panel: The crystallographic model of the FdGltS derivative obtained after reaction of C1 with 5-diazo-5-oxo-L-norleucine in complex with 2-OG is shown (PDB file: 1OFE). The enzyme domains are color coded as follows: blue, glutamine amidotransferase (GAT) domain, residues 1−478; red, central domain, residues 423−786; green, synthase/FMN domain, residues 787−1239; purple, C-terminal β-helix, residues 1240−1507. In the synthase domain FMN and the [3Fe-4S]$^{+1}$ cluster are shown as yellow sticks and as spacefill, respectively. The position of 2-OG (in sticks) is also indicated. In the GAT domain the positions of the C1-oxonorleucine (ONL) covalent adduct and of E1013 are shown. Right panel: Details of the same region of the GAT domain including residues of loop 4 of the synthase domain (thin lines, green) and of the central domain (thin lines, red) with S1011 and I1012 of loop 4 obstructing the tunnel entrance with T503 and N504 of the central domain. Distances, in angstroms, between selected atom pairs are shown. In the left panel, loop 4 of the synthase domain (residues 968−1013) and loop 471−504 of the central domain are shown as ribbons in the model of FdGltS. The dotted line indicates the path of the ammonia molecule from the site of release, beyond the constriction formed by residues 1011−1012 and 503−504 through the tunnel lined, on one side, by loop 4 residues, to reach 2-OG in the synthase site.

GltS is subjected to mechanisms of cross control of the glutaminase and synthase activities, as found in other amidotransferases (*2*−*7*). The enzyme is unable to hydrolyze L-Gln in the absence of both 2-OG and reducing equivalents at the synthase site. Furthermore, L-Gln hydrolysis, at the glutaminase site, is tightly coupled to L-Glu synthesis from 2-OG, at the synthase site, so that the rate of L-Glu production from L-Gln matches that of L-Glu produced from 2-OG. Finally, in FdGltS, reduced Fd in complex with the reduced enzyme is also required in order to activate the glutaminase site (*2*−*4*, Figure 1).

Comparison of the crystallographically determined structures of the single subunit of FdGltS (Figure 2) and of the homologous α subunit of NADPH-GltS showed that the structures of these enzymes are similar to each other (*8*−*10*). In all cases the ammonia tunnel connecting the glutaminase and synthase domain is fully formed, but it appears to be obstructed at the entry point (toward the glutaminase site) by main chain atoms of residues at the C-terminus of loop 4 of the synthase domain (residues 1011 and 1012 of loop 4 in FdGltS) and of the 423−786 loop of the so-called central domain (residues 503−504 in FdGltS, Figure 2). Furthermore, the Q-loop, conserved on all type II amidotransferases, which is believed to shield bound glutamine from solvent in order to prevent the escape of the released ammonia molecule from the glutaminase site, is in an open conformation in all available GltS structures. Thus, on the basis of GltS known catalytic and structural properties, the enzyme has been proposed to exist in at least two conformations, which differ for the fine structure of the glutaminase site and of the tunnel entrance.

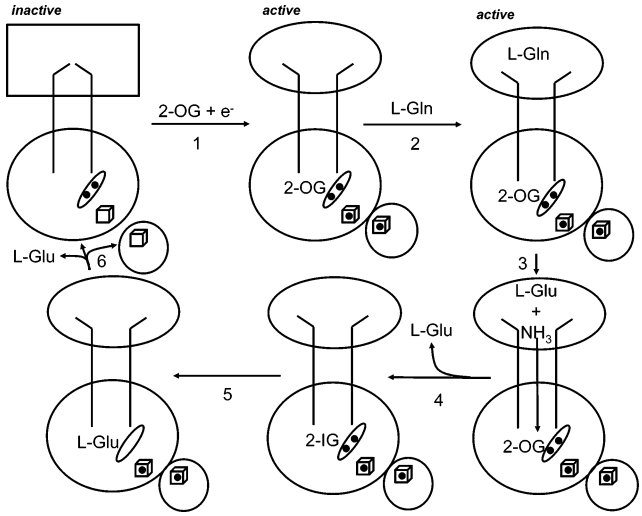

FIGURE 3: Minimal model for the activation of FdGltS glutaminase site effected by 2-OG binding and cofactor reduction in the synthase site. The enzyme consists of a catalytically competent synthase site (large circle) regardless of the ligation and redox state of the enzyme cofactors (FMN, oval; [3Fe-4S] cluster, cube). The glutaminase site (in the GAT domain) is proposed to exist in an inactive conformation (rectangle), which is converted to the active conformation (oval) upon 2-OG binding to the synthase site and reduction. 2-OG binding and cofactor reduction is also proposed to cause the opening of the ammonia tunnel entry point. In FdGltS, binding of reduced Fd to the 3-electron reduced enzyme (with FMN in the hydroquinone form and the reduced [3Fe-4S] cluster) seems required for activation (*13*).

As depicted in Figure 3, in the free enzyme, 2-OG may bind to the synthase site and the cofactors can be reduced. In this state the glutaminase site is in an inactive conforma-

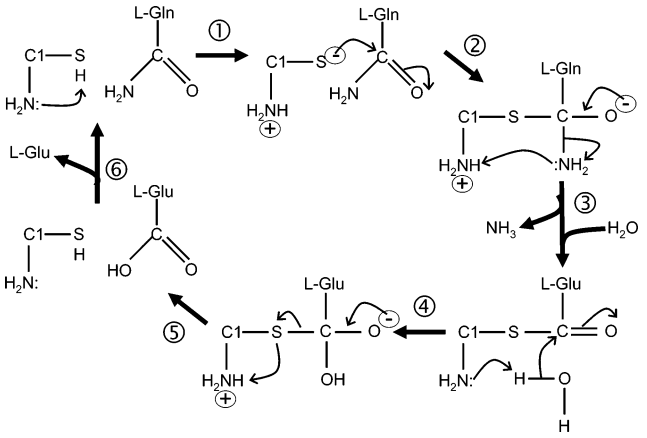

FIGURE 4: Proposed mechanism of the glutaminase reaction of type II amidotransferase. Step 1: Deprotonation of C1 thiol effected by the N-terminal amino group. Step 2: Formation of the first transient tetrahedral intermediate upon attack of C1 thiolate on L-Gln C(5) carbon favored by the oxyanion hole formed by Asn 227 side chain amide nitrogen atom and G228 backbone amide group. Step 3: Decay of the transient intermediate with release of ammonia, assisted by proton transfer from the N-terminal nucleophile, and formation of the Cys1-γ-glutamyl thioester intermediate. Step 4: Formation of the second transient tetrahedral intermediate, favored by the presence of the oxyanion hole and assisted by C1 free amino group. Step 5: Formation of the L-Glu product and (step 6) regeneration of the free enzyme.

tion that may bind glutamine, but is unable to hydrolyze it. 2-OG binding and cofactor reduction at the synthase site (as well as association with reduced Fd in the FdGltS) should induce limited but significant conformational changes that result in (i) activation of the glutaminase site toward glutamine hydrolysis and (ii) opening of the ammonia tunnel to promote ammonia diffusion to the synthase site with concomitant (iii) closure of the Q loop to prevent ammonia from escaping into the solvent. While crystallography failed to reveal the conformation of the enzyme at various stages of the catalytic cycle, it indicated which residues may be part of the mechanism of cross-control and coordination of activities of the GAT and synthase site (*2*−*4*). Among them, E1013 of FdGltS seems to be at a key position (Figure 2, right). This residue is conserved in all GltS and is at the C-terminus of loop 4 (residues 968−1013 of FdGltS) that emerges from the synthase domain, where it contacts residues involved in 2-OG binding and residues that interact directly with the redox cofactors. Loop 4 forms part of the wall of the ammonia tunnel and contributes with residues 1011 and 1012 to the constriction of the tunnel at the GAT end. E1013, which is the only residue of the synthase domain making contacts with residues of the glutaminase site, has been proposed to play a major role in activating glutamine hydrolysis and ammonia transfer through the tunnel in response to 2-OG binding and cofactor reduction at the synthase site (*2*−*4*).

Close inspection of the crystallographic structures of GltS shows how this residue may play multiple roles in the enzyme. In all FdGltS structures E1013 δ-carboxylate group appears to interact with the C1 α-amino group, which is the proposed active site base that participates in glutamine hydrolysis (Figure 4). E1013 also interacts with the R31 NH1 nitrogen, which, in turn, seems important for the correct positioning of C1 through an interaction with its main chain carboxylic oxygen atom. E1013 side chain carboxylate group may also interact with N227 amide nitrogen (Figure 2), which forms with G228 an oxyanion hole conserved in all type II amidotrasferases and believed to promote the formation of the covalent C1-γ-glutamyl thioester intermediate and its subsequent hydrolysis. Finally, E1013 side chain may also play a role in the precise geometry of the tunnel entry point. As shown in Figure 2 (right), one of its side chain oxygen atoms may interact with both E1013 main chain amide nitrogen and S1011 side chain hydroxyl group. Because of this network of interactions of E1013 at the C-terminus of loop 4 of the synthase domain, binding of 2-OG and cofactor reduction at the synthase site may induce small conformational changes to the glutaminase site that activate the reaction through repositioning of E1013 side chain. The same changes might cause the tunnel to open and favor ammonia transfer to the synthase site.

In order to test this hypothesis, E1013 was substituted with D, N, and A residues in FdGltS by site-directed mutagenesis of *gls*F, the gene encoding *Synechocystis* sp. PCC6803, cloned into a pUC18 derivative (*12*).

The wild-type FdGltS and the three protein variants were produced in *Escherichia coli* cells and purified to homogeneity with a similar purification procedure. Their characterization showed that the D, N, and A substitutions of E1013 led to enzyme forms altered with respect to their ability to hydrolyze L-glutamine, to the coupling between the glutaminase and the synthase reaction, and to their sensitivity to the presence of 2-OG and reducing equivalents at the synthase site. In particular, the E1013D/FdGltS variant revealed that L-Gln may participate in the activation of the glutaminase reaction of glutamate synthase during the catalytic cycle, completing the effect brought about by 2-OG binding and cofactor reduction at the synthase site.

EXPERIMENTAL PROCEDURES

Enzyme Production. Plasmid pFN14, a pUC18 derivative containing the 9.5 kb *Cla*I fragment of *Synechocystis* PCC603 DNA including the *gls*F gene, was used for the production of FdGltS (*11*). pFN14 was also used as the template in site-directed mutagenesis experiments designed to produce the E1013D, E1013N, and E1013A variants of FdGltS. The QuikChange site-directed mutagenesis kit (Stratagene) was employed according to manufacturer's instructions to obtain the desired pFN14-E1013D, pFN14-E1013N, and pFN14-E1013A plasmids. The same protocols were used for production and purification of wild-type enzyme and the E1013D, N, and A variants. *E. coli* CLR207 cells were transformed with pFN14 or its derivatives. Approximately 100 colonies of transformants, which were selected on Luria−Bertani (LB) plates containing 0.1 mg/mL ampicillin, were transferred to nine 2 L Erlenmeyer flasks containing 500 mL of LB broth supplemented with ampicillin (0.1 mg/mL) each. Cells were grown at 37 °C for 20 h under orbital shaking (220 rpm) without inducer. Cells were harvested by centrifugation and stored frozen until used for enzyme purification. Approximately 15 g of cells was resuspended in 30 mL of 50 mM imidazole/HCl buffer, pH 7.5, 1 mM EDTA, 1 mM 2-OG, 100 mM KCl and 1 mM phenylmethylsulfonyl fluoride. After sonication for a total of 5 min in a Branson Sonifier model 250 (output 35 W), and centrifugation at 18000 rpm for 60 min in a Sorval RC5C

centrifuge (SS34 rotor), protamine sulfate (0.3%, w/v) was added to the crude extract. Precipitated nucleic acids were removed by centrifugation at 15000 rpm for 10 min. The supernatant was slowly diluted 2-fold with 25 mM Hepes/KOH, pH 7.0, 1 mM EDTA, 1 mM 2-OG, 10% glycerol (buffer A) containing 2 M ammonium sulfate. After equilibration for approximately 30 min and removal of precipitated proteins by centrifugation at 15000 rpm for 10 min, the supernatant was loaded by gravity onto a Phenyl Sepharose High Performance column (1.6 cm × 10 cm, 20 mL) equilibrated with buffer A containing 1 M ammonium sulfate. Unbound proteins were removed by washing the column with 200 mL of equilibrating buffer. The column was then connected to an Akta (GE Healthcare) apparatus and developed at 1−1.5 mL/min by applying 1 column volume of buffer A containing 1 M ammonium sulfate, followed by a 200 mL linear gradient from 1 to 0 M ammonium sulfate in buffer A. FdGltS enriched fractions, which were found at approximately 0.5 M ammonium sulfate, were pooled, concentrated by ultrafiltration in an Amicon cell equipped with a YM30 membrane, and dialyzed overnight against 2 L of buffer A containing 1 mM DTT. The protein solution was then loaded onto a Q-Sepharose Fast Flow column (2.6 cm × 9.5 cm, 50 mL) equilibrated with buffer A. Unbound and weakly bound proteins were eluted by rinsing the column with the equilibration buffer and with the same buffer containing 0.1 M NaCl (100−150 mL) at 0.5 mL/min by gravity. The column was then connected to the Akta apparatus and developed at 1.3 mL/min by flowing buffer A containing 0.1 M NaCl (50 mL) followed by a gradient from 0.1 to 0.2 M NaCl in 50 mL and from 0.2 to 0.4 M NaCl in 250 mL. FdGltS eluted at approximately 0.3 M NaCl. Enzyme containing fractions were concentrated by ultrafiltration and loaded on a Ultrogel AcA34 column (2 cm × 80 cm, 190 mL) equilibrated and eluted with 25 mM Hepes/KOH buffer, pH 7.5, 1 mM EDTA, 1 mM 2-OG and 10% glycerol (buffer B) at 10 mL/h. FdGltS containing fractions were pooled on the basis of their A_{278}/A_{438} ratio (<8), concentrated by ultrafiltration, and dialyzed overnight against 2 L of buffer B containing 1 mM DTT. After centrifugation the enzyme was stored frozen at −80 °C after rapid freezing in liquid nitrogen. In some instances, SDS−PAGE analysis of the resulting sample showed the presence of two contaminating proteins of approximately 80 and 60 kDa, respectively, which could be removed by a second Phenyl-Sepharose chromatography using a small column (1.6 cm × 2.5 cm, 5 mL). During the entire purification procedure, the working temperature was 5 °C and buffers were equilibrated with nitrogen.

Production and Purification of Synechocystis PCC6803 Ferredoxin. Synechocystis PCC6803 ferredoxin was overproduced in *E. coli* DH5α cells transformed with pCK2 plasmid (*12*). Colonies of freshly transformed *E. coli* DH5α cells were transferred to 4−9 2 L Erlenmeyer flasks containing 500 mL of LB broth supplemented with 0.1 mg/mL ampicillin and 50 μM $FeSO_4$. After 20 h growth at 37 °C under orbital shaking, cells were harvested by centrifugation, washed with 10 mM Tris/HCl buffer, pH 8.0, 1 mM EDTA (TE buffer), and stored frozen. Typically, cells (8 g) were resuspended in TE buffer (16 mL) and subjected to five 1 min cycles of sonication. The crude extract was obtained by centrifugation after addition of 8 mL of TE buffer. The sample was loaded by gravity onto a Q-Sepharose Fast Flow column (1.6 cm × 10 cm, 20 mL) equilibrated with 25 mM Hepes/KOH buffer, pH 7.5 (buffer C). The column was rinsed with the equilibration buffer and buffer C containing 0.2 M NaCl, in the cold room. The column was then connected to the Akta apparatus and developed by applying a NaCl gradient from 0.2 to 0.4 M in 100 mL and from 0.4 to 0.6 M in 200 mL at 1.3 mL/min. Fd eluted at approximately 0.5 M NaCl. The Fd-containing fractions were pooled and slowly diluted 2-fold with buffer C containing 3 M ammonium sulfate. After equilibration on ice for 30 min, the sample was centrifuged to remove precipitated material and the supernatant was loaded onto a Phenyl Sepharose CL4B column (1.6 cm × 10 cm, 20 mL) equilibrated with buffer C containing 1.5 M ammonium sulfate. Under these conditions Fd is only retarded by the resin. When Fd was near the bottom, the column was connected to the Akta apparatus and a gradient from 1.5 to 0 M ammonium sulfate in buffer C in 200 mL was applied at a flow rate of 1 mL/min. Fractions were pooled on the basis of the A_{256}/A_{278} ratio (<0.9) in order to remove nucleic acids that at this stage seemed to be the main contaminants of the sample. After concentration by ultrafiltration in an Amicon cell equipped with a YM3 membrane, the Fd solution was gel filtered on a Sephadex G75 column (1.8 cm × 80 cm, 190 mL) equilibrated and eluted with buffer C. Fractions with a A_{256}/A_{278} ratio <0.8 were pooled and concentrated by ultrafiltration. Aliquots were stored at −80 °C after flash freezing in liquid nitrogen. Also during the purification of Fd, the temperature was kept at 5 °C and buffers were equilibrated with nitrogen.

Scheme 1: Summary of Catalytic Activities of FdGltS

L-[U-^{14}C]-Gln + 2-OG + Fd_{red} → L-[U-^{14}C]-Glu + L-Glu + Fd_{ox}	Fd-GltS activity
L-[U-^{14}C]-Gln + 2-OG + MV_{red} → L-[U-^{14}C]-Glu + L-Glu + MV_{ox}	MV-GltS activity
NH_3 + 2-[U-^{14}C]-OG + Fd_{red} → L-[U-^{14}C]-Glu + MV_{ox}	NH_3-dependent activity
L-[U-^{14}C]-Gln → L-[U-^{14}C]-Glu + NH_3	glutaminase activity
L-Glu + INT_{ox} → 2-OG + NH_3 + INT_{red}	L-Glu:INT oxidoreductase activity

Activity Assays. Glutamate:iodonitrotetrazolium Oxidoreductase Activity. The increase of absorbance at 490 nm of 1 mL reactions containing 0.1 mM iodonitrotetrazolium (INT), 20 mM L-Glu in 50 mM CAPS/KOH buffer, pH 9.5, was measured at 25 °C (*13*). An extinction coefficient of 18.5 mM^{-1} cm^{-1} was used to calculate the activity, which is expressed as μmol of INT reduced per min per μmol of enzyme (i.e.: apparent turnover number in min^{-1}).

Glutamate Synthase Activities. The physiological Fd-dependent glutamate synthase reaction (FdGltS activity, Scheme 1) was initially measured by incubating FdGltS forms (0.004 μM to 9 μM) in the presence of L-[U-^{14}C]-Gln (2.34 mM, 7290 dpm/nmol), 2-OG (2.5 mM), Fd (20 μM), dithionite (4 mM from a 100 mM stock solution in 25 mM Hepes/KOH buffer, pH 7.5, 1 mM EDTA, 10% glycerol that had been made anaerobic) in 50 mM Hepes/KOH buffer, pH 7.5, at 25 °C in 125−250 μL assays under anaerobiosis conditions as previously described (*13*). The assays were set up in reacti-vials sealed with a Teflon septum. Anaerobiosis was made by bubbling oxygen-free nitrogen for 20 min into the assay mixture lacking proteins and dithionite, which were added in rapid succession through the Teflon septum with gastight Hamilton microsyringes to start the reaction. The assay was kept at 25 °C in the dark with nitrogen flowing

on the solution surface for 20 min, after which an aliquot (100 μL) was withdrawn and loaded onto a 1 mL Dowex 1X8 column (acetate form) equilibrated in water and eluted with 6 × 1 mL aliquots of water, 8 × 1 mL of 0.3 M acetic acid, and 6 × 1 mL aliquots of 1 M acetic acid. Either fractions were individually collected in pico-vials (Packard) or the water, 0.3 M acetic acid, and 1 M acetic acid eluates were separately pooled and counted. Quantification of the radioactive species was done with a Packard Tri-Carb 2 100TR scintillation counter using Ultima Gold (Packard) as the scintillation fluid. Under these conditions residual L-Gln was recovered in the water fractions, L-Glu in the 0.3 M acetic acid fractions, and part of 2-OG in the 1 M acetic acid wash. The latter was detected when 2-[U-^{14}C]-OG (2.5 mM, 8178 dpm/nmol) was used instead of ^{14}C-labeled L-Gln to monitor GltS activity.

To measure initial velocities of reactions, 300−600 μL assays were set up. At different times (typically 4, 8, 12, and 20 min for assay setup and, later, 3, 6, and 9 min) 70−140 μL aliquots were withdrawn and 50 or 100 μL were loaded on the Dowex 1X8 columns for quantification of L-[U-^{14}C]-Glu formed from L-[U-^{14}C]-Gln or 2-[U-^{14}C]-OG. The enzyme concentration used in the assays was determined in order to obtain a linear increase of L-Glu concentration for at least 5−10 min. The nmol of L-Glu formed in the 50 or 100 μL aliquots were plotted as a function of time (in min), and the activity was calculated from the slope of the best fit of the initial data to a straight line. All activities are expressed as apparent turnover number in min^{-1} to normalize for protein concentration.

In order to determine the values of the apparent Michaelis constant (K_M) for the enzyme substrates and maximum velocity (expressed as apparent turnover number, k_{cat}, in min^{-1}), L-Gln or 2-OG concentrations were varied as detailed in the relevant tables or figures.

The Grafit 4.0 software package (Erythacus Software Ltd) was used to fit the initial velocity values (v) as a function of the varied substrate concentration (S) to the Michaelis−Menten (eq 1), Lineweaver−Burk (eq 2), or Hill equation (eq 3) and to obtain the values and the associated errors of the steady-state kinetic parameters. K is K_M in eq 1 and 2 and the value of the concentration of substrate at which v equals half of the maximum velocity (V) in eq 3. In eq 3, n is the Hill coefficient (*14*).

$$v = (V \times S)/(K + S) \quad (1)$$

$$v = 1/V + (K/V)(1/S) \quad (2)$$

$$v = (V \times S^n)/(K + S^n) \quad (3)$$

A similar scheme was used to measure the methylviologen (MV)-dependent glutamate synthase reaction (MV-GltS activity, Scheme 1) except for the substitution of Fd with 0.4 mM MV (from a 10 mM stock in water). MV was added to the reaction mixture prior to equilibration with oxygen-free nitrogen.

The ammonia-dependent glutamate synthase activity was measured anaerobically in the presence of ferredoxin and dithionite as described above, with the following modifications: (i) assays were run in 50 mM CHES/KOH buffer, pH 9.3; (ii) 2-[U-^{14}C]-OG was used (2.5 mM, 8178 dpm/nmol) in the presence of (iii) ammonium chloride (100 mM from a 1 M NH_4Cl stock at pH 9.3) as the ammonia donor.

Glutaminase Activity. To measure the glutaminase activity of GltS, reaction mixtures were similar to those described above, but Fd (or MV), dithionite, and 2-OG were omitted. The assays were carried out in the presence of oxygen.

pH Dependence of Glutamate Synthase Activity. The pH dependence of the initial velocity of the Fd-dependent glutamate synthase reaction was measured at fixed substrates concentrations (2.34 mM L-Gln, 2.5 mM 2-OG, and 20 μM Fd) in 50 mM Hepes/KOH buffers adjusted to pH values between 7.0 and 8.5. The ionic strength of the assays was kept constant at 50 mM with KCl.

The initial velocity values as a function of pH were fitted to eqs 4 and 5 (*14*). Equation 4 describes the case in which activity decreases from a maximum limiting value (V) at high pH as one group dissociates. Equation 5 describes the case in which activity increases as one group dissociates to reach a maximum, pH independent value (V).

$$v = (V \times 10^{pH-pK_a})/(10^{pH-pK_a} + 1) \quad (4)$$

$$v = (V \times 10^{pK_a-pH})/(10^{pK_a-pH} + 1) \quad (5)$$

Fd-Sepharose Affinity Column and Study of the Fd/FdGltS Interaction. Synechocystis sp PCC6803 Fd was covalently linked to Sepharose 4B using the method described in ref *15*. The resin (1 mL) was packed in a C10/10 column (GE Healthcare) and connected to the Akta apparatus. The column was equilibrated with 25 mM Hepes/KOH buffer, pH 7.5. 200 μL of FdGltS (0.1−0.2 mg) was injected onto the column, which was developed by flowing 2 mL of equilibrating buffer followed by a NaCl gradient from 0 to 1.0 M in the same buffer in 10 mL. The flow rate was 0.1 mL/min, and the absorbance at 280 nm of the eluate was recorded continuously.

Attempts To Trap the Enzyme γ-Glutamyl Thioester Intermediate. In order to attempt to trap the postulated γ-glutamyl thioester intermediate (Figure 4) the wild-type enzyme and the E1013D/N/A variants (9 μM, 1.5 mg/mL) were incubated with L-[U-^{14}C]-Gln (2.34 mM, 7292−50000 dpm/nmol) alone or, anaerobically, under turnover conditions in the presence of 2-OG (2.5 mM), Fd (20 μM), and dithionite (4 mM) in 50 mM Hepes/KOH buffer, pH 7.5, in 150 μL, as described for activity assays. In order to obtain separation between the enzyme and free L-Gln two methods were used. In the first case centrifugal gel filtration was used (*16*). 0.5 and 10 min after the addition of the enzyme to the reaction mixture equilibrated at at 25 °C, 50 μL aliquots of the solutions were withdrawn and loaded onto Bio-Spin columns (BioRad) containing Bio-Gel P6 that had been equilibrated with 100 mM Hepes/KOH buffer, pH 7.5. The column was subjected to centrifugation at 1000*g* for 1 min in the cold room in a Heraeus Labofuge 400 centrifuge equipped with a 8172 swing-out rotor. The column was rinsed 5 × 50 μL aliquots of equilibrating buffer followed by 7 × 100 μL and 2 × 200 μL aliquots. Fractions were collected in Eppendorf tubes. 20 μL of each fraction were counted, and 5−10 μL aliquots were used to determine their protein content with the Bradford Reagent (Amresco). As controls, mixtures lacking L-[U-^{14}C]-Gln or the enzyme, or containing BSA (1.5 mg/mL) or NADPH-GltS (9 μM)

Table 1: Catalytic Activities of Wild-Type FdGltS and the E1013D/N/A Variants

activity	initial velocity, min^{-1}			
	FdGltS	FdGltS/E1013D	FdGltS/E1013N	FdGltS/E1013A
Fd-dependent glutamate synthase[a]	3356 ± 400	19 ± 5	0.60 ± 0.18	0.25 ± 0.10
MV-dependent glutamate synthase[a]	86.7 ± 7.4	12.7 ± 0.4	0.27 ± 0.04	0.32 ± 0.02
NH_3-dependent glutamate synthase[b]	130 ± 3.0	140.8 ± 20	110 ± 10	128 ± 6.1
glutaminase[c]	94.2 ± 2.7	3.1 ± 0.04	0.13 ± 0.06	0.11 ± 0.04
L-Glu:INT oxidoreductase[d]	220 ± 4.0	203 ± 2.4	284 ± 4.5	188 ± 0.8

[a] Wild-type and E1013D/N and A variants of FdGltS (0.009−9 μM) were incubated anaerobically with L-[U-^{14}C]-Gln (2.34 mM, 7300 dpm/nmol), 2-OG (2.5 mM), Fd (20 μM) or MV (0.4 mM), dithionite (4 mM) in 50 mM Hepes/KOH buffer, pH 7.5. At different times, 50 μL aliquots were chromatographed on 1 mL Dowex 1X8 (acetate form) columns, which were eluted with water, 0.3 M CH_3COOH, 1 M CH_3COOH. L-Glu was found in the 0.3 M CH_3COOH eluate. The initial velocities were calculated from plots of nmol of L-Glu formed as a function of the incubation time. [b] For the NH_3-dependent reaction L-Gln was substituted by NH_4Cl (0.1 M). 2-[U-^{14}C]-OG (2.5 mM, 8200 dpm/nmol) and 50 mM CHES/KOH, pH 9.3 were used. [c] The glutaminase reaction was measured in the presence of L-[U-^{14}C]-Gln alone. [d] The L-Glu:INT oxidoreductase activity was assayed spectrophotometrically by measuring the initial velocity of reduction of INT (0.1 mM) at 490 nm in the presence of L-Glu (20 mM) in 50 mM CAPS/KOH buffer, pH 9.5, at 25 °C.

instead of FdGltS, were treated as described above. Under these conditions, greater than 90% of the applied protein eluted in the first 3 fractions, well separated from free L-[U-^{14}C]-Gln that was recovered in fractions 5−10. The second method of separation consisted of trichloroacetic acid (TCA) precipitation of the protein. In this case 400 μL incubation mixtures were set up. At different times 150 μL aliquots were added to cold 150 μL of 20% (w/v) TCA. The samples were incubated for 30 min on ice. The protein was recovered by centrifugation in a minifuge at 13000 rpm for 10 min and 4 °C. The pellet was washed 2 times with 1 mL aliquots of an acetone:1 M HCl mixture (48/1 acetone/HCl ratio) and recovered after each rinse by centrifugation. After drying in a Speed-Vac the final pellet was transferred to a scintillation vial containing 1 mL of Ultima Gold scintillation fluid, and the ^{14}C content was determined by scintillation counting. As a control BSA (1.5 mg/mL) was substituted for FdGltS.

Miscellaneous Techniques. Absorbance spectra were recorded with a HP8453 diode-array spectrophotometer. Spectrophotometric activity assays were carried out using Cary 219 or Cary 100 (Varian) spectrophotometers. Flavin and iron content as well as the extinction coefficients of the proteins were determined as previously described (*13*, *17*).

RESULTS

General Properties of FdGltS E1013D/N/A Variants. The wild-type FdGltS and its E1013D/N/A variants could be overproduced in *E. coli* CLR207 cells at similar levels. The same purification procedure allowed us to obtain 0.5−1 mg per gram of cell paste of homogeneous preparations of the four enzyme species with 20−25% yields. Throughout the purification the enzyme was quantified by measuring the L-Glu:INT oxidoreductase activity (Scheme 1), which takes place within the synthase site (Figure 1, *13*). The wild-type enzyme and the E1013D/N/A FdGltS variants showed similar behavior and yields during all chromatographic steps and similar L-Glu:INT oxidoreductase specific activities at all purification steps. The values of the final preparations were also similar, ranging from 1.1 to 1.3 U/mg in different preparations. The absorbance spectra of the final enzyme preparations were indistinguishable from each other with maxima at 278, 369, and 438 nm and minima at 328 and 384 nm, and A_{278}/A_{438} ratios between 7.5 and 8. The calculated extinction coefficients at 438 nm of 26.5 ± 1.5 mM^{-1} cm^{-1} for FdGltS/E1013D, 26.0 ± 2.0 mM^{-1} cm^{-1} for FdGltS/E1013N, and 25.0 ± 1.0 mM^{-1} cm^{-1} for FdGltS/E1013A compare well with that determined for the wild-type enzyme (24.4 mM^{-1} cm^{-1}, *13*). Furthermore, the FdGltS variants showed a behavior similar to that of the wild-type enzyme also during sulfite titrations of the FMN cofactor and anaerobic reductive titrations with dithionite (not shown).

Catalytic Properties of FdGltS E1013D/N/A Variants. The physiological Fd-dependent glutamate synthase activities (Scheme 1) of the wild-type enzyme and of the FdGltS E1013D/N/A variants were initially determined by measuring the initial velocity of production of L-[U-^{14}C]-Glu in anaerobic reaction mixtures as described in the Experimental Procedures section and in the legend of Table 1. Under these conditions, the turnover number of FdGltS was 3356 min^{-1}. The E1013D substitution was found to cause a ∼150-fold decrease in activity, while the E1013N and E1013A FdGltS variants exhibited a ∼5000−10000-fold lower activity than the wild-type enzyme.

When MV was substituted for Fd in the assay mixtures as the reductant, the glutamate synthase activity of wild-type FdGltS was approximately 40-fold lower than that measured in the presence of ferredoxin, confirming the stimulatory effect of bound reduced Fd on the glutamate synthase reaction (*13*). The MV-dependent activities of the E1013D and E1013N variants were approximately 2-fold lower than the corresponding Fd-dependent reaction, while for FdGltS/E1013A this activity was very low and similar to that measured with Fd. The glutaminase activity of FdGltS was similar to the MV-dependent activity. Also this activity was significantly affected in the E1013D/N/A variants decreasing to ∼3 min^{-1} for the E1013D variant and to barely detectable levels for the E1013N and E1013A FdGltS forms. On the contrary the NH_3-dependent glutamate synthase activity and the L-Glu:INT oxidoreductase reactions, which solely involve the synthase site, appeared unaffected by the amino acyl substitutions. The lack of effect of the E1013D/N/A substitutions on the properties of the synthase site was confirmed by determining the apparent maximum velocity (V) and K_M values for L-Glu and INT for the L-Glu:INT oxidoreductase reaction (Table 2). This finding, together with the unaltered redox and sulfite reactivity of the protein variants, rules out that the E1013 substitutions have a significant effect on the redox properties of the enzyme cofactors bound at the synthase site.

Table 2: Comparison of the Steady-State Kinetic Parameters of the L-Glutamate:INT Oxidoreductase Activity Exhibited by Wild-Type and E1013D/N and A Variants of FdGltS[a]

FdGltS	L-Glu, mM	INT, mM	V, min^{-1}	K_{L-Glu}, mM	K_{INT}, mM	V/K_{L-Glu}, mM^{-1} min^{-1}
wild-type	0.05−2	0.2	220 ± 4	0.044 ± 0.005		5000 ± 575
	1	0.07−0.5	366 ± 14		0.12 ± 0.010	
E1013D	0.05−1	0.2	203 ± 2.4	0.059 ± 0.0025		3440 ± 151
	0.2	0.05−1	376 ± 6		0.14 ± 0.008	
E1013N	0.05−1	0.2	284 ± 4.5	0.045 ± 0.003		6311 ± 433
	0.2	0.05−1	337 ± 5		0.10 ± 0.006	
E1013A	0.05−1	0.2	188 ± 0.8	0.019 ± 0.0005		9741 ± 256
	0.2	0.05−1	200 ± 3		0.09 ± 0.005	

[a] Assays were carried out spectrophotometrically at 25 °C in CAPS/KOH buffer, pH 9.5 (50 mM) and at the stated substrate concentrations or concentration ranges.

Furthermore, the lack of effect of the amino acyl substitutions on the activities that do not involve the glutaminase site indicates that the E1013 substitutions specifically affected the catalytic properties of the glutaminase site of FdGltS.

In order to test if the low Fd-dependent glutamate synthase activity of the E1013D/N/A variants and the low stimulation of the velocity of glutamate synthesis from L-Gln brought about by Fd, as compared to the reaction in the presence of MV, might be due to an effect of the E1013 substitutions on the interaction between the enzyme forms and Fd, we measured the Fd-dependent glutamate synthase activity of the four protein forms in the presence of 10 and 40 μM Fd. The initial velocities of the reactions were essentially identical to those measured in the presence of 20 μM Fd (not shown) indicating that the amino acyl substitutions had not caused a significant increase of the apparent K_M value for reduced ferredoxin. That the E1013D/N/A substitutions had no detectable effect on the Fd/FdGltS interaction was also tested by affinity chromatography. This method has been recently used, for example, to establish the binding affinity of various ferredoxins to *Toxoplasma gondii* ferredoxin:NADP$^+$ reductase (*15*) in that the NaCl concentration needed to elute the enzyme from the Fd-Sepharose affinity column correlates with the dissociation constant of the Fd/enzyme complex. Affinity chromatography was adopted to investigate the interaction between Fd and FdGltS instead of direct absorbance- or fluorescence-monitored titrations because the observed changes of the signal brought about by addition of Fd were found to be too small to give any reliable indication of binding due to the high background absorbance (or fluorescence) of free FdGltS. FdGltS was found to bind to the resin and to elute when NaCl concentration in the buffer was 0.44 M. Similar results were obtained by chromatographing the E1013D/N/A variants under identical conditions, demonstrating that the E1013 substitutions had no detectable effect on the binding interaction with Fd. In control experiments also the interactions between *Synechocystis* Fd and NADPH-GltS and its α subunit were studied. These proteins did not bind to Fd-Sepharose, confirming the specificity of the Fd/FdGltS interaction.

pH Dependence of the Fd-Dependent Glutamate Synthase Activity of FdGltS and Effect of the E1013D/N/A Substitutions. The hypothesis that the decrease of glutamate synthase activity observed on removal of the carboxylate group of E1013 from the glutaminase site of FdGltS could be due to an effect of E1013 substitutions on the pH dependence of the reaction velocity was tested. Because of the difficulty to carry out anaerobic and discontinuous activity assays, initial velocities were measured at fixed concentrations of all reagents at pH values between 7 and 8.5, where the enzyme and Fd are stable. The initial velocities of the reaction catalyzed by wild-type FdGltS decreased as the pH increased (Figure 5). The data are reasonably described by a curve that assumes that the velocity decreases as a group with a pK_a of 8.6 dissociates (Figure 5). The trends of initial velocities of reactions catalyzed by the E1013D and E1013N variants of FdGltS as a function of pH were similar to each other and increased at increasing pH with an apparent pK_a of ~6.5−6.8. However, the absolute initial velocity values of the E1013D variant were ~40-fold higher than those of the E1013N/FdGltS form when activity was monitored with radiolabeled L-Gln, reflecting the differences of activity measured at pH 7.5 (Table 1).

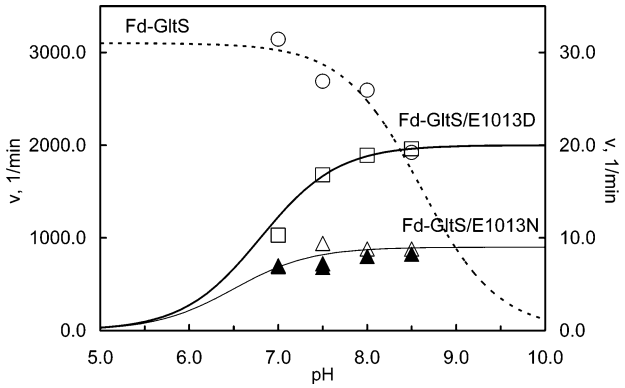

FIGURE 5: pH dependence of the glutamate synthase reaction catalyzed by wild type and E1013D/N and A variants of FdGltS. Open symbols: Initial velocities of reactions containing L-[U-^{14}C]-Gln (2.34 mM, 7300 dpm/nmol), 2-OG (2.5 mM), Fd (20 μM), sodium dithionite (4 mM) in 50 mM Hepes/KOH buffer at the indicated pH values were determined using wild-type FdGltS (circles, left axis), the E1013D (squares) and the E1013N variant (triangles). Closed triangles: Initial velocities of reactions in the presence of L-Gln (2.5 mM) and 2-[U-^{14}C]-OG (2.5 mM, 8200 dpm/nmol) and the E1013N FdGltS variant. The values obtained with the wild-type enzyme are plotted using the left axis; those obtained with the E1013D FdGltS variant are plotted using the right axis; the values obtained with the E1013N variant and L-[U-^{14}C]-Gln have been multiplied by 20 and those obtained with 2-[U-^{14}C]-OG by 40, and the right axis is used. The dotted line shows the theoretical curve obtained by assuming that the reaction velocity of wild-type FdGltS decreases from an upper value of 3100 min^{-1} as a group with a pK_a value of 8.6 dissociates. The thick line through the E1013D FdGltS data shows the expected curve if the reaction velocity increases to an upper value of 20 as a group with pK_a value of 6.8 dissociates. The line through the E1013N data (triangles) shows the theoretical curve that describes the case in which the reaction velocity increases to an upper value of 9 as a group with pK_a value of 6.5 dissociates.

Experiments were not done with the E1013A FdGltS variant because of the low activity. The data collected here are not sufficient to make hypotheses on the identity of residues whose protonation state is important for substrate binding or catalysis in the wild-type FdGltS and in its variants. However, the different pH dependence of the activity of the wild-type enzyme as opposed to the E1013 variants can be explained by taking into account that the E1013 substitutions mainly affect the glutaminase segment of the overall reaction so that it is not surprising that the protonation state of different groups governs the reaction in the wild-type and mutant enzmes. On the other hand, the similar pH dependence observed with the E/D and E/N variants suggests that the negative charge of the 1013 residue does not influence the acid−base properties of the glutaminase active site and, at the same time, reinforces the concept that the glutaminase reaction determines to a great extent the measured turnover with these FdGltS variants. For practical purposes, the main conclusion that can be drawn from these measurements is that, in spite of the fact that the pH profile of FdGltS activity is dramatically altered by the E1013 substitutions, kinetic analyses of wild-type and mutant forms of FdGltS can be carried out at pH 7.5 where the enzyme is stable, and, from this experiment, the pH is reasonably close to the optimal value for all enzyme species.

Effect of E1013 Substitutions on the Kinetic Parameters of FdGltS Reaction. In order to establish if the low activity measured for the glutamate synthase and glutaminase reactions of the E1013D/N/A variants of FdGltS is mainly due to an effect of the amino acyl substitutions on substrate binding or to an effect on following steps of the glutaminase reaction, we measured the kinetic parameters of the Fd-dependent glutamate synthase reaction for all the four enzyme forms. Because of the technical difficulty of carrying out the anaerobic and radioactive assays of this reaction, measurements were done at constant Fd concentration (20 μM) in the presence of a fixed concentration of L-glutamine (or 2-OG) and varied concentrations of the second substrate.

The initial velocities of reactions with the wild-type FdGltS showed hyperbolic dependence on both L-glutamine and 2-OG concentrations (Figure 6, top, Table 3). The K_{2-OG} value determined in the presence of 2.36 mM L-Gln (100 μM) is approximately 10-fold lower than that reported previously (*3*, *11*), but only 5-fold higher than the K_d value determined spectrophotometrically during backtitrations of the FdGltS/sulfite complex (17.4 μM, *13*). The K_{L-Gln} (2.4 mM), which was determined in the presence of saturating 2-OG (2.34 mM), was instead similar to that previously reported (2.5 mM, *3*, *11*).

When reactions were carried out using 2-[U-^{14}C]-OG instead of L-[U-^{14}C]-Gln, the initial velocities were essentially identical to those obtained using radiolabeled L-Gln, confirming that glutamine hydrolysis at the glutaminase site is tightly coupled to L-glutamate synthesis from 2-OG at the synthase site in wild-type FdGltS, with a 1:1 stoichiometry of glutamine hydrolyzed at the glutaminase site and L-Glu formed from 2-OG at the synthase site.

Under similar conditions, similar initial velocities were measured using either radiolabeled L-Gln or radiolabeled 2-OG with the E1013D variant of FdGltS, demonstrating that also in this enzyme form the glutaminase and synthase reactions are tightly coupled (Figure 6, middle). It was also confirmed that the maximum velocity of the reaction is approximately 2 orders of magnitude lower than that measured with the wild-type enzyme (Figure 6, Table 3). The dependence of the initial reaction velocity on 2-OG concentration was hyperbolic although with a K_{2-OG} higher than that measured with the wild-type enzyme. On the contrary, the initial velocities obtained at varying L-Gln concentrations and 2.5 mM or 5 mM 2-OG revealed that the data were better described by a sigmoid function (eq 3), as also confirmed by double reciprocal plots that showed a deviation from linearity at low L-Gln concentrations (Figure 7). When 2-OG concentration was lowered to 0.25 mM, the data were reasonably fitted with a hyperbole with a deviation from linearity of the double reciprocal plot (Figure 7) only at the lowest L-Gln concentration used. The K_{L-Gln} value estimated from the linear part of the double reciprocal plot (Figure 7) was approximately 10 mM, only 5-fold higher than that determined with the wild-type enzyme.

With the E1013N FdGltS variant the dependencies of initial reaction velocities on L-Gln or 2-OG concentrations were hyperbolic (Figure 6, bottom). However, the values obtained using L-[U-^{14}C]-Gln were systematically approximately twice those obtained with 2-[U-^{14}C]-OG as the radiolabeled substrate, confirming the results obtained during the study of the pH dependence of the activity (Figure 5). The calculated K_{2-OG} values were only 2−4-fold higher than those measured with the wild-type enzyme. The K_{L-Gln} value was of the same order of magnitude as that measured for the wild-type enzyme regardless of the radiolabeled substrate used. It was confirmed that the maximum velocity with L-[U-^{14}C]-Gln, at saturating 2-OG concentration, is almost 4 orders of magnitude lower than that of the wild-type enzyme.

While the origin of the sigmoid kinetics observed with the E1013D variant of FdGltS will be discussed in the Discussion section, it is confirmed here that the E1013 substitutions have a significant effect on the maximum velocity of the reaction, but affect the K_M values for the substrates only to a limited extent. Although the K_M is not always a direct measure of the dissociation constant of the enzyme−substrate complex, the measured values strongly indicate that the E1013D and N substitutions do not dramatically weaken glutamine binding to the enzyme. Removal of the net negative charge carried by either E or D leads to partial uncoupling of the glutaminase and synthase reactions of FdGltS, besides causing the observed dramatic drop in maximum velocity. This conclusion was confirmed with the E1013A FdGltS variant. Because of its low activity the determination of the steady-state kinetic parameters of the reaction catalyzed by this enzyme form could not be carried out. However, at fixed L-Gln and 2-OG concentrations (2.5 mM each), the initial reaction velocity was 0.125 min^{-1} with radiolabeled L-Gln and below detection with ^{14}C-labeled 2-OG, with 9.5 μM enzyme in parallel assays. This result indicates that in the E1013A variant of FdGltS the glutaminase and synthase sites are even less coupled than in the E1013N enzyme form.

Attempts To Trap the γ-Glutamyl Thioester Intermediate in the Wild-Type and E1013D, N, and A FdGltS Species. The decrease of activity measured with the E/D and the E/N

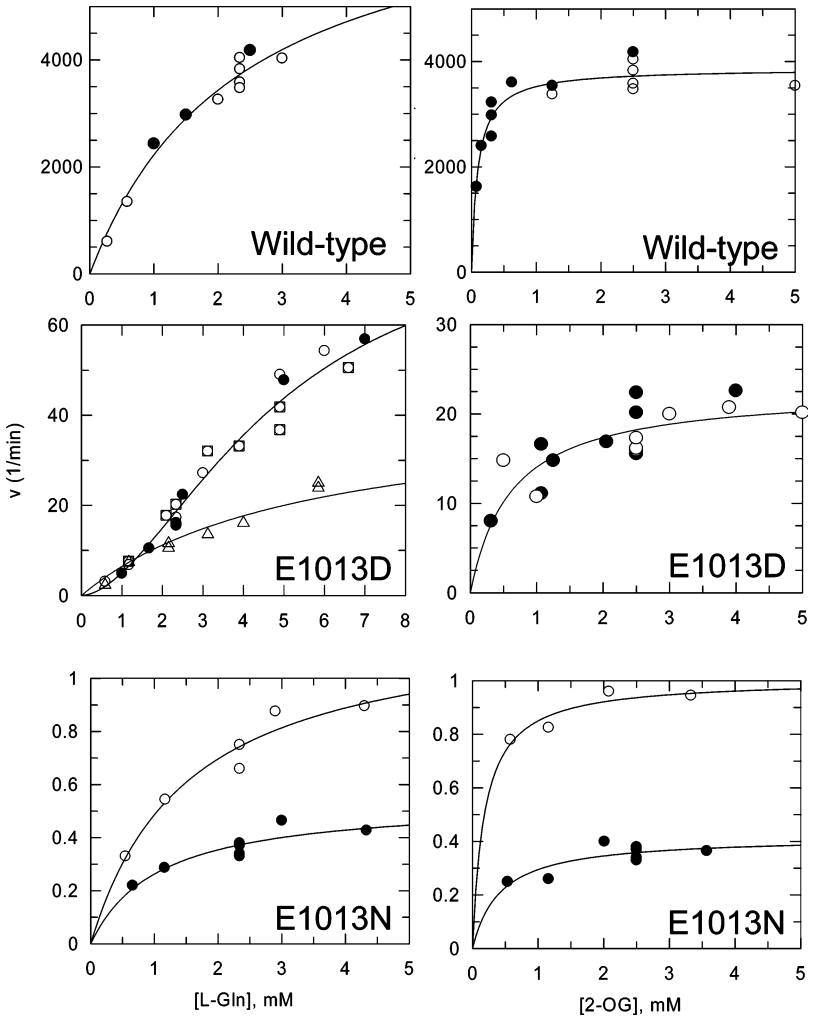

FIGURE 6: Steady-state kinetic analyses of the FdGltS E1013D/N/A variants. Reactions were carried out in 50 mM Hepes/KOH buffer, pH 7.5 in the presence of 21 μM Fd, 4 mM sodium dithionite, and FdGltS (19 nM, top), FdGltS/E1013D (2 μM, middle), or FdGltS/E1013N (4 μM, bottom). The amount of L-Glu formed from L-[U-^{14}C]-Gln (open symbols) or 2-[U-^{14}C]-OG (closed symbols) was determined after chromatography on Dowex 1X8 of 100 μL aliquots of the reaction mixtures withdrawn at 1, 3, 6, 9 min. Circles: The concentration of the fixed substrate was 2.5 mM (2-OG) or 2.34 mM (L-Gln). With FdGltS/E1013D, assays at varying L-Gln concentration were also carried out in the presence of 0.25 mM (triangles) and 5 mM 2-OG (squares). The curves shown correspond to the best fit of the data to the Michaelis−Menten equation except for the center left panel, which shows the fit to the Hill equation.

Table 3: Summary of the Steady-State Kinetic Parameters Calculated for the Wild-Type and the E1013D and E1013N Forms of FdGltS[a]

enzyme	2-OG, mM	L-Gln, mM	eq	V (min^{-1})	K_{2-OG}, mM	K_{L-Gln}, mM	n
wild-type	2.34	0.6−3	1	7508 ± 1145		2.4 ± 0.7	
	0.080−10.0	2.5	1	3868 ± 106	0.098 ± 0.019		
E1013D	2.5 and 5[b]	0.58−7.0[b]	3	84 ± 9.3[b]		15.6 ± 1.7[b]	1.75 ± 0.17[b]
	2.5 and 5[c]	2.5−7.0[c]	2	128 ± 46[c]		9.6 ± 3.8[c]	
	0.25[c]	0.58−5.85[c]	2	42 ± 9[c]		5.5 ± 1.2[c]	
	0.31−5	2.5	1	22.7 ± 2.24	0.62 ± 0.25		
E1013N	2.34	0.54−4.3 (^{14}C)[d]	1	1.23 ± 0.14		1.52 ± 0.45	
	2.34 (^{14}C)[d]	0.66−4.3	1	0.54 ± 0.06		1.06 ± 0.39	
	0.58−3.33	2.5 (^{14}C)[d]	1	1.01 ± 0.05	0.18 ± 0.064		
	0.53−3.6 (^{14}C)[d]	2.5	1	0.42 ± 0.035	0.42 ± 0.18		

[a] Assays were carried out in 50 mM Hepes/KOH buffer, pH 7.5, at 25 °C as described in the legend of Table 1. The data are shown in Figures 6 and 7. [b] The complete datasets obtained with 2.5 and 5 mM 2-OG were fitted together to the Hill equation (eq 3, Figure 6). [c] After inspection of double reciprocal plots (Figure 7) the reciprocal velocity values that showed a linear dependence on the reciprocal of L-Gln concentration were fitted to eq 2. The errors of the estimated parameters V and K were calculated according to Bevington (*20*). [d] The radiolabeled substrate used is indicated.

FdGltS variants, in the absence of effects on the properties of the synthase site, supported the hypothesis that the negative charge contributed by the δ-carboxylate group of E1013 is important for catalysis of the glutaminase segment of the FdGltS reaction. Determination of the kinetic parameters of the reaction catalyzed by the FdGltS variants also indicated that the E/D and E/N substitutions had a limited effect on L-Gln binding but a dramatic effect on the maximum velocity. Because of E1013 position in the glutaminase site (Figure 2) this residue may be important to

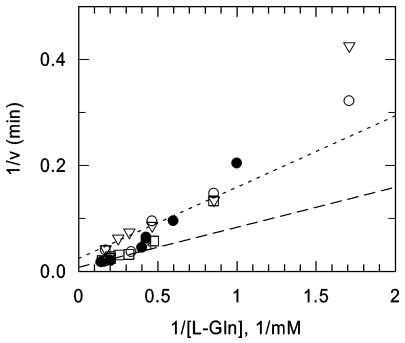

FIGURE 7: Nonlinear double reciprocal plot of FdGltS/E1013D at varied L-Gln and fixed 2-OG. The reciprocal values of initial velocity of reactions catalyzed by FdGltS/E1013D in the presence of varying L-Gln and fixed concentrations of 2-OG (squares, 5 mM; circles, 2.5 mM; triangles, 0.25 mM, see Figure 6) are plotted as a function of the reciprocal of L-Gln concentration. The dashed line is the best fit of the data obtained at L-Gln concentration greater than 2.5 mM at 2.5 mM and 5 mM 2-OG with eq 2. The dotted line is the best fit to eq 2 of the data obtained at L-Gln concentrations greater than 1 mM with 0.25 mM 2-OG. The calculated kinetic parameters *V* and *K* are in Table 3. Open symbols, data obtained with L-[U-^{14}C]-Gln; closed symbols, data obtained with 2-[U-^{14}C]-OG.

assist the hydrolysis of the enzyme γ-glutamyl thioester intermediate (Figure 4, step 4). If this step had been selectively slowed down by the amino acyl substitutions, in the E1013D and, especially, the E1013N and E1013A variants of FdGltS, the reaction velocity might be limited by the hydrolysis of the intermediate, and the low rate of decay of this species might allow us to isolate it. Therefore, the wild-type and the three E1013 variants of FdGltS were incubated with L-[U-^{14}C]-glutamine alone or under turnover conditions and the proteins were rapidly separated from free L-[U-^{14}C]-glutamine by either centrifugal chromatography or TCA precipitation. The levels of radioactivity associated with the wild-type and mutant enzymes were similar to each other and never exceeded a stoichiometry of 0.01 mol of ligand per mol of enzyme. These results rule out a *specific* effect of E1013 substitutions on the hydrolysis of the γ-glutamyl thioester intermediate. Rather, it must be concluded that, regardless of which step(s) is (are) affected by the amino acyl substitutions, also in the E1013D, N, and A FdGltS variants the rate of hydrolysis of the covalent intermediate is significantly faster than that of formation.

DISCUSSION

As detailed in the introduction, E1013 belongs to loop 4 of FdGltS and is the only residue of the synthase domain engaged in a number of interactions with residues of the glutaminase site of the enzyme (Figure 2, right panel). Therefore, the hypothesis was made that small, but significant, conformational changes that alter the position of E1013 in the FdGltS glutaminase site may be part of the mechanism of activation of the glutaminase reaction as a function of the ligation and redox state of the synthase site during the catalytic cycle (Figure 3). Furthermore, E1013 may determine the geometry of the entry point of the ammonia tunnel by interacting with its backbone nitrogen and S1011 side chain hydroxyl (Figure 2, right).

Substitutions of E1013 with D, N, and A residues confirmed the role of E1013 in various properties of FdGltS, which will be discussed separately for clarity.

The amino acyl replacements had no detectable effect on the activities associated with the synthase site, namely, the ammonia-dependent reaction and the L-Glu:INT oxidoreductase activity, nor on the interaction with Fd, confining their effect to the properties of the glutaminase site and of the ammonia tunnel.

Both the glutaminase and the glutamate synthase activities decreased of about 2 orders of magnitude with the E/D substitution and almost 4 orders of magnitude with the E/N replacement even at saturating L-Gln concentrations indicating that both substitutions mainly affect the glutaminase segment of the GltS reaction and that it is the net negative charge of E1013 that is important for the catalysis of glutamine hydrolysis in FdGltS. Since the E1013 substitutions have a limited effect on the K_M value for L-Gln (Figure 6, Table 3), E1013 does not seem to play a major role in glutamine binding. The low reaction rate may be due to a role of E1013 substitutions on the acidity of the C1 α-amino group, the N-terminal nucleophile, to disruption of the oxyanion hole through removal of the interaction between E1013 and N227 amide nitrogen, or, less specifically, to an altered overall geometry of the glutaminase site. The experiments presented here, which are limited by both the low activities of the E1013 variants and the difficulties of the discontinuous and anaerobic assays, do not allow to distinguish among the hypotheses. However, the pH dependencies of the initial velocities of the FdGltS reaction catalyzed by the E1013D and E1013N variants are similar to each other, regardless of the radiolabeled substrate used to monitor the reaction, arguing against a direct or indirect role of the residue in acid−base catalysis of the glutaminase reaction. Furthermore, we were unable to isolate the γ-glutamyl thioester intermediate ruling out that the FdGltS variants are trapped as the covalent intermediate. With this in mind, one would favor the hypothesis that E1013 is important either for the precise geometry of the glutaminase site or, more interestingly, for the formation of the oxyanion hole through its interaction with N227 amide nitrogen. However, addressing these issues would require a detailed analysis of the kinetics and mechanism of the glutaminase reaction, which was outside the scope of the present work.

In the wild-type enzyme and in the E1013D variant of FdGltS the velocity of production of L-Glu from L-[U-^{14}C]-Gln and that from 2-[U-^{14}C]-OG are essentially the same under all conditions tested (Figure 6), while with the E1013N and the E1013A variants the rate of glutamine hydrolysis is at least twice that of production of L-Glu from 2-OG at the synthase site (Figure 5 and 6, Table 3). These results confirm that in the wild-type FdGltS the glutaminase and synthase sites are tightly coupled (i.e.: with a 1:1 stoichiometry of L-Glu produced from L-Gln and L-Glu from 2-OG) and show how the negatively charged carboxylate group of E1013 (or D1013 in the E1013D variant) is sufficient to maintain coupling. Coupling requires that when 2-OG is bound at the synthase site, the cofactors are reduced and reduced Fd is bound, the catalytically competent conformation of the glutaminase site is obtained and, at the same time, the tunnel entrance widens to promote ammonia transfer to the synthase site. The higher rate of glutamate production from L-Gln than that from 2-OG in the E/N and E/A protein variants is consistent with a role of E1013 in ensuring opening of the tunnel entrance. E1013 is suitably positioned to interact with

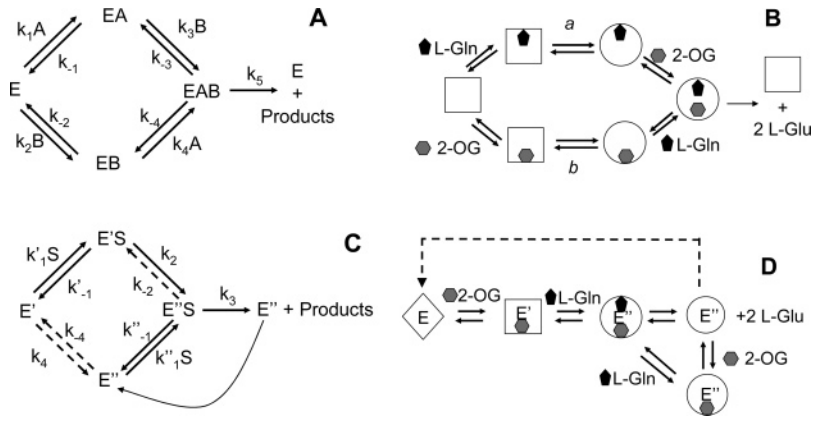

FIGURE 8: Schemes consistent with the sigmoidicity exhibited by the dependence of initial velocity on L-glutamine concentration by FdGltS/E1013D. Panel A: Nonequilibrium random bireactant system (*14*). Panel B: Application of the general mechanism of panel A to FdGltS. Panel C: Substrate-induced enzyme isomerization under non-rapid equilibrium conditions giving rise to sigmoid activity versus substrate concentration curves (*18*) and application to FdGltS (panel D).

its own backbone N atom and with S1011 side chain hydroxyl potentially forming H bonds in which one of the E1013 carboxylate oxygens is the donor (Figure 2, right). Shortening of the side chain at this position with the E1013D substitution may maintain these interactions, while substitution of the negatively charged E or D δ (or γ)-carboxylate with the neutral carbamide side chain of N may abolish them. A third requirement for coupling between the glutaminase and the synthase sites is that the glutaminase site is shielded from solvent so that ammonia cannot diffuse into the solvent. E1013 does not seem to be sufficiently close to residues of the Q loop (residues 216−231) to affect its conformation.

Unexpectedly, with the E1013D substitution, a sigmoid dependence of the initial velocity of reactions upon L-Gln concentration was observed at 2.5 and 5 mM 2-OG. At low (0.25 mM) 2-OG the activity versus L-glutamine curve was instead mainly hyperbolic (Figures 6 and 7).

This finding is consistent with the hypothesis that the glutaminase site exists in at least two conformations (Figure 3) and, interestingly, reveals a role of glutamine in the activation of the GltS glutaminase site. As depicted in Figure 3, it has been proposed that binding of 2-OG to the synthase site (as well as cofactor reduction and association with reduced Fd) may induce a change in the glutaminase site, through loop 4 residues including E1013, which stabilizes its fully active conformation. In the native enzyme, 2-OG binding, cofactor reduction, and association with reduced Fd seem sufficient to determine the full transition between the inactive and active conformations of the glutaminase site yielding a hyperbolic dependence of reaction velocity upon L-Gln concentration. The sigmoid kinetics observed with the E1013D FdGltS variant suggest that when D replaces E1013, the communication between the synthase and glutaminase sites is less efficient and the ligation state of the synthase site may cause GltS to exist in a conformational equilibrium between the inactive and active conformations of its glutaminase site. Binding of L-Gln appears to shift the equilibrium toward the active conformation. The two species do not seem to differ dramatically for their affinity for L-Gln, but for the velocity at which L-glutamine is hydrolyzed.

While the allosteric effect of 2-OG (and of the other ligands of the synthase site, which will not be mentioned any longer in the following discussion for simplicity, i.e.: electrons loaded on the cofactors and bound reduced Fd) may take place in the isolated FdGltS monomer, the interpretation of the sigmoid kinetics observed with L-Gln does not necessarily require the presence of FdGltS dimers. The aggregation state of GltS is still a matter of active investigation. While gel filtration chromatography and small-angle X-ray scattering experiments showed that FdGltS is a monomer in solution, the asymmetric unit of FdGltS crystals contains a dimer of identical subunits and oligomers have been detected by mass spectrometry (*2*−*4*). However, sigmoid velocity-versus-substrate curves can be observed in monomeric enzymes, as reviewed in ref *14*, whenever the expression of initial velocity is in the form of eq 6, where *i*, *j*, *k*, *l*, and *m* are combinations of rate constants, with $im > jl$ and $ki > mj$.

$$v/[E]_t = (i[S]^2 + j[S])/(k + l[S]^2 + m[S]) \qquad (6)$$

Cases that originate sigmoid curves are observed in random bi bi systems if the rapid equilibrium conditions do not apply and one route to the central complex leading to products is kinetically more favorable than the other as depicted in Figure 8A. If this were the case with FdGltS, one could postulate that what makes one branch kinetically favored over the other is the rate of isomerization of the enzyme from the inactive to the active conformation of the glutaminase site when 2-OG binds to the synthase site. In the wild-type enzyme, 2-OG binding would induce a fast conversion, making the reaction proceed only through the lower branch of the kinetic scheme (Figure 8B) that implies binding of 2-OG, rapid conversion to the fully active form and binding of L-Gln with L-Gln hydrolysis (and/or subsequent steps) being the slow step in the process. In the E1013D variant, the isomerization step induced by 2-OG binding to the free enzyme may have become extremely slow. However, when 2-OG binds to the enzyme−L-Gln complex, the conformational change may be faster. As a result, a branched kinetic scheme like the one depicted in Figure 8A,B would become operative with the E1013D enzyme species, with the lower branch of the path being the kinetically unfavored one. At fixed 2-OG concentrations, partitioning between the lower (kinetically unfavored) and upper (favored) branches of the pathway would depend on L-Gln concentration yielding the observed hyperbolic kinet-

ics. However, if this scheme were operative, when 2-OG is varied in the presence of subsaturating L-Gln, the velocity would initially increase hyperbolically to a maximum value at a given concentration of 2-OG. At higher 2-OG concentrations substrate inhibition is expected because the kinetically unfavored (lower) branch of the path would become operative. This was not observed in our experiments (Figure 6).

An alternative, and attractive, explanation is the one depicted in Figure 8C,D. It can be demonstrated that if a single substrate-single site enzyme can exist in two forms and steady-state rather than rapid equilibrium conditions prevail, the expression of initial velocity as a function of substrate concentration will be in the form of eq 6 (*14*). As described in ref *18* for the scheme of Figure 8C to apply, and to give rise to sigmoid kinetics, the interconversion of the E′ and E″ states, whether free or in complex with the substrate, must be slow relative to all other reaction steps. Furthermore, the E′ ↔ E″ isomerization should be very slow and kinetically negligible, the E′S → E″S conversion should be the rate-limiting step of the reaction, and k_3 should be much greater than k_{-2}. Finally, E′ should be thermodynamically more stable than E″. In this case, the concentration of the E″S complex depends on the concentration of E′S, thus on that of S. Since at the end of each catalytic cycle E″ does not convert back to E′, after the first turnover the slow isomerization step is bypassed and the actual concentration of the catalytically relevant species (E″ + E″S) is set. It can be proposed that, in the wild-type FdGltS, the conversion of E to E″ is fast and hyperbolic kinetics are observed. In the E1013D FdGltS variant, binding of 2-OG to the free enzyme (E) would (slowly) convert the glutaminase site into the E′ state to which L-Gln may bind inducing the isomerization to E″ (Figure 8D). Low concentrations of 2-OG would cause the E ↔ E′ equilibrium to be shifted toward E and, perhaps, make the conversion of E″ into E kinetically significant. As a result, the enzyme would cycle between E and E″ (the linear sequence of reaction steps of Figure 8D with the cycle closed by the broken arrow) yielding hyperbolic kinetics as a function of L-Gln concentration. At high 2-OG concentrations, the level of E″ depends on L-Gln concentration that converts E′ into E″, and the E″ → E interconversion becomes negligible leading to the observed sigmoid kinetics.

Thus, it can be proposed that in FdGltS both 2-OG (with the other "ligands" of the synthase site, namely, the cofactors in the reduced state and the bound reduced ferredoxin) and L-Gln may contribute to the activation of the glutaminase site and to ammonia transfer through the tunnel, in a two-step process that requires partial activation upon binding of 2-OG (and cofactors reduction) at the synthase site, followed by full activation brought about by glutamine binding. This two-step activation process is masked in the wild-type enzyme. Interestingly, a two-step activation process involving ligands of the synthase site and glutamine has been recently proposed on the basis of crystallographic structures of various forms of glucosamine 6-phosphate synthase, an amidotransferase that shares with GltS the homologous type II amidotransferase domain (*19*). Also in this case, one residue of the synthase domain (T606) is involved in the signaling pathway. This similarity, in spite of the fact that these enzymes are formed by homologous amidotransferase domains but unrelated synthase domains, may support the proposal that amidotransferases can be viewed as a case of convergent evolution (*2*).

ACKNOWLEDGMENT

We thank Drs. A. Mattevi and R. H. H. van den Heuvel for providing the plasmids for the production of the E1013 variants of FdGltS used in this study, Dr. A. Freddi for technical assistance, Drs. G. Zanetti, A. Aliverti, and A. Pennati for advice for the preparation of Fd and the Fd-Sepharose affinity column, and Drs. J. Blanchard and P. Cook for helpful discussions.

REFERENCES

1. Vanoni, M. A., and Curti, B. (1999) Glutamate synthase: a complex iron-sulfur flavoprotein, *Cell. Mol. Life Sci. 55*, 617−638.
2. van den Heuvel, R. H. H., Curti, B., Vanoni, M. A., and Mattevi, A. (2004) Glutamate synthase: a fascinating pathway from L-glutamine to L-glutamate, *Cell. Mol. Life Sci. 61*, 669−681.
3. Vanoni, M. A., Dossena, L., van den Heuvel, R. H. H., and Curti, B. (2005) Structure-function studies on the complex iron-sulfur flavoprotein glutamate synthase: the key enzyme of ammonia assimilation, *Photosynth. Res. 83*, 219−238.
4. Vanoni, M. A., and Curti, B. (2005) Structure-function studies on the iron-sulfur flavoenzyme glutamate synthase: an unexpectedly complex self-regulated enzyme, *Arch. Biochem. Biophys. 433*, 193−211.
5. Zalkin, H., and Smith, J. (1998) Enzymes utilizing glutamine as the amide donor, *Adv. Enzymol. Relat. Areas Mol. Biol. 72*, 87−143.
6. Massière, F., and Badet-Denison, M.-A. (1998) The mechanism of glutamine amidotransferases, *Cell. Mol. Life Sci. 54*, 205−222.
7. Raushel, F. M., Thoden, J. B., and Holden, H. (2003) Enzymes with molecular tunnels, *Acc. Chem. Res. 36*, 539−548.
8. Binda, C., Bossi, R. T., Wakatsuki, S., Artz, S., Coda, A., Curti, B., Vanoni, M. A., and Mattevi, A. (2000) Cross-talk and ammonia channeling between active centers in the unexpected domain arrangement of glutamate synthase, *Structure 8*, 1299−1308.
9. van den Heuvel, R. H. H., Ferrari, D., Bossi, R. T., Ravasio, S., Curti, B., Vanoni, M. A., Florencio, F. J., and Mattevi, A. (2002) Structural studies on the synchronization of catalytic centers in glutamate synthase, *J. Biol. Chem. 277*, 24579−24583.
10. van den Heuvel, R. H. H., Svergun, D. I., Petoukhov, M. V., Coda, A., Curti, B., Ravasio, S., Vanoni, M. A., and Mattevi, A. (2003) The active conformation of glutamate synthase and its binding to ferredoxin, *J. Mol. Biol. 330*, 113−128.
11. Navarro, F., Martin-Figueroa, E., Candau, P., and Florencio, F. J. (2000) Ferredoxin-dependent iron-sulfur flavoprotein glutamate synthase (GlsF) from the cyanobacterium *Synechocystis* sp. PCC 6803: Expression and assembly in *Escherichia coli*, *Arch. Biochem. Biophys. 379*, 267−276.
12. Schmitz, S., Navarro, F., Kutki, C. K., Florencio, F. J., and Boehme, H. (1996) Glutamate 94 of [2Fe-2S] -ferredoxins is important for efficient electron transfer in the 1:1 complex formed with ferredoxin-glutamate synthase (GltS) from *Synechocystis* sp. PCC 6803, *Biochim. Biophys. Acta 1277*, 135−140.
13. Ravasio, S., Dossena, L., Martin-Figueroa, E., Florencio, J, F., Mattevi, A., Morandi, P., Curti, B., and Vanoni, M. A. (2002) Properties of the recombinant ferredoxin-dependent glutamate synthase of *Synechocystis* PCC6803. Comparison with the *Azospirillum brasilense* NADPH-dependent enzyme and its isolated α subunit, *Biochemistry 41*, 8120−8133.
14. Segel, I. H. (1975) in *Enzyme kinetics*, Wiley & Sons, New York.
15. Pandini, V., Caprini, G., Tedeschi, G., Seeber, F., Zanetti, G., and Aliverti, A. (2006) Roles of the species-specific subdomain and the N-terminal peptide of *Toxoplasma gondii* ferredoxin-$NADP^+$ reductase in ferredoxin binding, *Biochemistry 45*, 3563−3571.
16. Penefsky, H. S. (1977) Reversible binding of Pi by beef heart mitochondrial adenosine triphosphatase, *J. Biol. Chem. 252*, 2891−2899.

17. Aliverti, A., Curti, B., and Vanoni, M. A. (1999) Identifying and quantitating FAD and FMN in simple and iron-sulfur-containing flaviproteins, in *Methods in Molecular Biology, Flavoprotein Protocols* (Chapman, S. K., and Reid, G. A., Eds.), Vol. 131, pp 9−23, Humana Press Inc., Totowa.
18. Rabin, B. R. (1967) Co-operative effects in enzyme catalysis: a possible kinetic model based on substrate-induced conformation isomerization, *Biochem. J. 102*, 22C−23C.
19. Mouilleron, S., Badet-Denisot, M. A., and Golinelli-Pimpaneau, B. (2006) Glutamine binding opens the ammonia channel and activates glucosamine-6P synthase, *J. Biol. Chem. 281*, 4404−4412.
20. Bevington, P.H. (1969) in *Data Reduction and error analysis for the physical sciences*, McGraw-Hill Inc., New York.

BI061865D